

Strengths and Limitations of SAFT for Calculating Polar Copolymer–Solvent Phase Behavior

BRUCE M. HASCH, SANG-HO LEE, and MARK A. MCHUGH*

Department of Chemical Engineering, Johns Hopkins University, Baltimore, Maryland 21218

SYNOPSIS

Statistical associating fluid theory (SAFT) is used to calculate the cloud-point behavior of poly(ethylene-co-methyl acrylate) (EMA) copolymers (0–41 mol % methyl acrylate) in ethane, propane, butane, ethylene, propylene, 1-butene, chlorodifluoromethane, and dimethyl ether at temperatures to 250°C and pressures to 2,600 bar. Poor agreement is obtained between calculated and experimental data if the pure component EMA parameters used in SAFT are calculated using mixing rules that average polyethylene (PE) and poly(methyl acrylate) (PMA) parameters. Therefore, two of the three pure component parameters for all of the EMA copolymers are fixed to the values reported for PE and the third parameter, u°/k , for the copolymer containing 31 mol % methyl acrylate (EMA₃₁) is determined by fitting the EMA₃₁–butane cloud-point curve. The value for $(u^{\circ}/k)_{\text{PMA}}$ is then obtained using a mixing rule and the values of u°/k for all of the EMA copolymers are calculated. A good fit of all of the copolymer–solvent cloud-point curves is obtained using a temperature-independent mixture parameter, k_{ij} . With this method of calculation it is possible to correlate cloud-point data with the SAFT equation of state if a small amount of experimental data are available. © 1996 John Wiley & Sons, Inc.

INTRODUCTION

In the last 20 years, a new class of ethylene copolymers has been developed that incorporates polar or hydrogen bonding groups into the backbone of polyethylene (PE). These ethylene-based copolymers are typically produced via free radical copolymerization at pressures in the range of 2,000–3,000 bar, and at temperatures as high as 250°C.¹ The physical properties of these copolymers vary not only with molecular weight and degree of chain branching, but also with polar comonomer content. When producing these copolymers it is important to know the location of the phase boundaries for copolymer–solvent mixtures to avoid potential fouling problems or runaway reactions that may occur if a two-phase region is allowed to form inside the reactor. However, predicting the phase behavior of these copolymer–solvent mixtures is a nontrivial proce-

sure, especially if the comonomer can hydrogen bond to itself or if it can form a complex with the solvent or cosolvent.

In this article the statistical associating fluid theory (SAFT) is used to calculate high-pressure copolymer–solvent phase behavior. SAFT is a perturbation-theory based equation of state developed by Chapman and colleagues² who applied the theory of associating fluids developed by Wertheim.^{3–6} Molecules are represented as covalently bonded chains of segments that may contain sites capable of forming associative complexes. In SAFT, the reference equation consists of terms accounting for the connectivity of the hard segments in the main chain, the hard-sphere repulsion of the segments, and the energy of site–site specific interactions of the segments with themselves or other segments; the perturbation term consists of a mean-field attractive term. With this approach, the residual Helmholtz free energy, a^{res} , relative to the ideal gas reference state is

* To whom correspondence should be addressed.

$$a^{\text{res}} = (a^{\text{hs}} + a^{\text{chain}} + a^{\text{assoc}}) + a^{\text{disp}} \quad (1)$$

Table I Physical Properties of Polymers Used

Polymer	MA (mol %)	M_n	M_w	M_w/M_n	% Crystallinity	T_{melt} (°C)
PE	0	20,100	106,000	5.1	42.0	123.0
EMA ₁₀	10	17,000	74,800	4.4	15.1	86.0
EMA ₃₁	31	33,000	108,900	3.3	~ 0	—
EMA ₄₁	41	42,000	110,400	2.6	~ 0	—

where a^{hs} is the Helmholtz free energy contribution of segment–segment, hard-sphere repulsion; a^{chain} is the Helmholtz free energy contribution of connectiveness of the segments (i.e., covalent bonds between segments); a^{assoc} is the Helmholtz free energy contribution for site–site specific interactions (i.e., hydrogen bonds); and a^{disp} is the Helmholtz free energy contribution of the mean-field, dispersion attraction between segments.

A body of work has recently been developed that uses SAFT to calculate the phase behavior of associating and nonassociating polymer–solvent systems. Chen and coworkers have published extensive work on nonhydrogen bonding, polyolefin–solvent mixtures,^{7–9} and hydroxy-terminated polymer–solvent mixtures.^{10,11} In addition to the studies by Chen et al., Beckman and coworkers¹² have shown that SAFT does a reasonably good job of predicting the phase behavior of nylon 6 + trifluoroethanol + CO₂ systems; and Hasch and McHugh¹³ have shown that SAFT is capable of modeling the cloud-point behavior of poly(ethylene-*co*-acrylic acid)–solvent mixtures. It is important to recognize that the majority of these prior studies applied the SAFT equation to polymer–solvent systems that were comprised of nonpolar polymers or modestly polar copolymers capable of forming hydrogen-bonded complexes. Recently, Pradhan and coworkers¹⁴ used SAFT to calculate the solubility and distribution coefficient of polystyrene in ethane and in propane. However, they used unrealistic values of the pure component parameters to correlate the experimental data. Pradhan et al.¹⁴ state that the parameters “are only first pass empirical estimates that do not have quantitative physical meaning.” In the present work we extend the ideas of Pradhan and colleagues¹⁴ for estimating the pure component parameters of different copolymers to demonstrate the utility of the SAFT equation for calculating the phase behavior of polar copolymer–solvent mixtures. Our approach provides a technique for correlating the phase behavior of copolymer–solvent mixtures if a small amount of cloud-point data is available.

In this study the SAFT equation is used to model the cloud-point behavior of binary mixtures of statistically random poly(ethylene-*co*-methyl acrylate) (EMA) copolymers with nonpolar ethane, propane, and butane; slightly polar ethylene, propylene, and butene; and highly polar dimethyl ether (DME) and chlorodifluoromethane (CDFM). The EMA copolymers have methyl acrylate contents of zero (PE), 10 (EMA₁₀), 31 (EMA₃₁), and 41 mol % (EMA₄₁); molecular weights and polydispersities as given in Table I. Although the major focus of this work is the modeling of these copolymer–solvent systems, an original set of data are presented for the EMA₃₁–DME system. The experimental technique used to obtain these data is given elsewhere¹⁵ and is not presented here.

SAFT

Because SAFT views a molecule as a number of segments connected in a chain, it is necessary to determine the contributions of hard-sphere repulsion, chain connectivity, and dispersion interactions to the equation of state. It is also necessary to determine the contributions to SAFT associated with hydrogen bonding and complex formation at specific sites on a molecule. In eq. (1), the residual Helmholtz free energy for the hard-sphere repulsion of a segment, a^{hs} , is obtained from the expression of Carnahan and Starling.¹⁶ The term for the energy of association or complex formation, a^{assoc} , is determined using an expression derived by Chapman and coworkers^{2,17} based on the associating fluid theory of Wertheim.^{3–6} The chain connectivity term, a^{chain} , also given by Chapman and coworkers, was obtained assuming very strong associative interactions between spheres that comprise a given molecule, thus simulating the contribution due to covalent bonding. The mean-field term, a^{disp} , is given by a power series derived by Alder et al.¹⁸ that is identical to that used in the perturbed hard chain theory of Beret and Prausnitz.¹⁹ The Helmholtz free energy expressions,

Table II Pure Component Parameters Used with SAFT Equation²⁰

Component	v^{oo} (cm ³ /mol)	m	u^o/k (K)	ϵ/k (K)	v (cm ³ /mol)
Ethane	14.460	1.941	191.44	0	0
Ethylene	18.157	1.464	212.06	0	0
Propane	13.457	2.696	193.03	0	0
Propylene	15.648	2.223	213.90	0	0
<i>n</i> -Butane	12.599	3.458	195.11	0	0
1-Butene	13.154	3.162	202.49	0	0
Dimethyl ether	11.536	2.799	207.83	0	0
CDFM	9.988	2.908	188.91	0 ^a	0 ^a

^a CDFM can form cross-associative complexes with the methyl acrylate groups in EMA. For these cross associations, $\epsilon/k = 1258.1$ K and $v = 0.152$ cm³/mol.

both for pure components and mixtures, are given in detail by Huang and Radosz^{20,21} and are not reproduced here.

The expression for the residual Helmholtz free energy is used, along with thermodynamic definitions, to derive an equation for the fugacity coefficient, ϕ_i , that is needed to calculate phase equilibria. This procedure has been explained in detail elsewhere.¹³

For each pure component there are potentially five parameters in the SAFT equation: v^{oo} , the temperature-independent volume of a segment; u^o/k , the temperature-independent, nonspecific energy of attraction between two segments; m , the number of segments in a molecule; ϵ/k , the energy of association between sites on a molecule; and v , the volume of site-site association. The parameters ϵ/k and v are nonzero only for hydrogen-bonding molecules. Three mixing rules are required for the extension of SAFT to mixtures: one for the temperature-dependent volume of a segment, v^o ; another for the temperature-dependent energy of attraction between two segments, u ; and a third one for the average segment size for the mixture, m . The mixing rule for the volume of a segment is

$$v^o = \frac{\sum_i \sum_j x_i x_j m_i m_j v_{ij}^o}{[\sum_i x_i m_i]^2} \quad (2)$$

where

$$v_{ij}^o = \frac{1}{8} [v_i^{o1/3} + v_j^{o1/3}]^3. \quad (3)$$

The mixing rule for the energy of attraction between segments is

$$\frac{u}{kT} = \frac{\sum_i \sum_j x_i x_j m_i m_j \left[\frac{u_{ij}}{kT} \right] v_{ij}^o}{\sum_i \sum_j x_i x_j m_i m_j v_{ij}^o} \quad (4)$$

where

$$u_{ij} = (u_{ii} u_{jj})^{1/2} (1 - k_{ij}). \quad (5)$$

The parameter k_{ij} is a fitted, binary mixture parameter that corrects the mean-field energy contribution to SAFT. The mixing rule for the average segment size for the mixture is

$$m = \sum_i \sum_j x_i x_j m_{ij} \quad (6)$$

where

$$m_{ij} = \frac{1}{2} (m_i + m_j). \quad (7)$$

A second mixture parameter could have been applied to either eq. (3) or (7) as suggested by Huang and Radosz.²¹ However, the fit of the experimental data was not significantly improved when two mixture parameters are used. In addition, each of these two mixture parameters had similar effects on the calculated fit; and therefore, only a single mixture parameter is used in the following presentation of results.

Table II lists values for the pure component parameters v^{oo} , u^o/k , and m for ethane, ethylene, propane, propylene, butane, 1-butene, and DME reported by Huang and Radosz.²⁰ Also shown in Table II are the pure component parameters for CDFM as determined from a fit of the SAFT equation to the CDFM vapor pressure curve and saturated liquid

Table III SAFT Parameters Calculated from Mixing Rules

Component	v_{oo} (cm ³ /mol)	m	u^o/k (K)	ϵ/k (K)	v (cm ³ /mol)
PE	12.00	1,024.3	216.15	0	0
EMA ₁₀	12.62	825.0	233.66	0	0
EMA ₃₁	14.00	1,432.7	271.17	0	0
EMA ₄₁	14.71	1,225.3	289.75	0	0
PMA	20.00	532.4	422.74	0	0

Pure component parameters for PMA obtained from a fit of pure component volumetric data.

densities data to temperatures within 30°C of the critical point of the pure CDFM. It should be noted that although the calculated critical temperatures for the nine solvents listed in Table II differ from the actual values by less than 5%, the calculated critical pressures can be as much as 18% greater than the experimental value.

Because pure component pressure–volume–temperature (PVT) data are not available for the EMA copolymers, these parameters must be calculated. In many copolymer–solvent calculational studies, the copolymer properties are determined with mixing rules that combine parameters of the two homopolymers that comprise the copolymer.²² The mixing rules used for these calculations are similar to eqs. (2)–(7), except that now they are applied to the two homopolymers that comprise the copolymer rather than to the two components in the mixture. The cross-terms used when applying eqs. (2)–(7) for copolymer pure-component calculations are listed in eqs. (8)–(10).

$$v_{E-MA}^{oo} = \frac{1}{8} [v_E^{oo1/3} + v_{MA}^{oo1/3}]^3, \quad (8)$$

$$\left(\frac{u^o}{k}\right)_{E-MA} = \left[\left(\frac{u^o}{k}\right)_E \cdot \left(\frac{u^o}{k}\right)_{MA} \right]^{1/2}, \quad (9)$$

and

$$m_{E-MA} = \frac{1}{2}(m_E + m_{MA}), \quad (10)$$

where the subscript E represents the pure-component parameters of PE and the subscript MA represents the pure-component parameters of poly(methyl acrylate) (PMA). Note that no “copolymer” adjustable parameters, such as k_{AB} , appear in eqs. (9) or (10), as suggested by Panayiotou²² who found that phase behavior calculations involving copolymer blends were quite sensitive to small changes in k_{AB} . However, the copolymer–solvent calculations considered here are much less sensitive to changes in k_{AB} ; and therefore, the use of an ad-

justable parameters for calculating copolymer pure component parameters is not warranted.

SAFT calculations are performed assuming that the copolymer molecular weight and chemical composition are “monodisperse,” because previous studies^{23,24} have shown that the effect of molecular weight and distribution is small compared to the effect of comonomer concentration. The cloud-point curves are obtained by calculating pressure–composition (P - x) isotherms at various temperatures. The calculated cloud-point pressure is the pressure at 5 wt % copolymer on the P - x isotherm.

Two different methods are used to generate pure component parameters for the EMA copolymers using the mixing rules described above. In the first method, density data²⁵ for PMA are fit to the SAFT equation to obtain the pure component parameters, then the mixing rules are used along with the pure component parameters of PE to calculate copolymer parameters²² as shown in Table III. The pure component PMA densities predicted using these parameters are within 3% of the values determined by Rodgers.²⁵ Unfortunately, a very poor fit of EMA–solvent cloud-point curves is obtained with these copolymer parameters. In fact, the calculated cloud-point curves are not even in qualitative agreement with experimental data as some of the calculated cloud-point curves are 1,000 bar too high in pressure. Also, while the experimentally determined cloud-point curves depend strongly on temperature, the calculated cloud-point curves show virtually no temperature dependence. Even a large, negative value for k_{ij} is unable to bring the calculations into reasonable agreement with the experiment. In hindsight, these results are not particularly surprising given that Huang and Radosz²⁰ correlated the pure component parameters for PE rather than determining them from a fit of density data, because efforts to calculate phase behavior using fitted PE parameters were unsuccessful. Because the parameters for PE were determined by correlation, copolymer parameters for EMA calculated by a combination

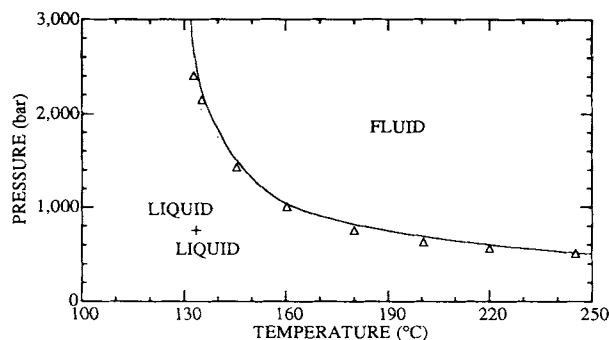


Figure 1 Calculated cloud-point curves for EMA₃₁ in butane with $u^\circ/k = 220$ K and $k_{ij} = 0.026$ compared to experimental data.²⁸ The symbols represent experimental data; the lines represent calculations obtained using SAFT.

of fitted PMA parameters and correlated PE parameters are internally inconsistent, and are unlikely to yield accurate predictions of the phase behavior. As a result, the parameters for PMA fitted to density data are not used to calculate the phase behavior of EMA-solvent mixtures.

For the second method used to determine EMA parameters, v^{oo} is fixed at 12 cm³/mol and m is calculated from $0.05096 \times$ number-average molecular weight (M_n), the same value and relationship used for PE. A value for $(u^\circ/k)_{\text{EMA}_{31}}$ is determined by fitting a single EMA₃₁-solvent cloud-point curve. With these simplifications the mixing rules for v^{oo} and m are now trivial, as $v^{oo} = 12$ cm³/mol and $m = 0.05096 \cdot M_n$ for all of the copolymers considered here, regardless of their backbone composition. The value of $(u^\circ/k)_{\text{PMA}}$ is now calculated from the previously determined value of $(u^\circ/k)_{\text{EMA}_{31}}$ using eq. (9) and the mixing rule given in eq. (4). With this calculated value of $(u^\circ/k)_{\text{PMA}}$, the values of u°/k for all of the copolymers can be calculated using eqs. (4) and (9). Although with this approach it is possible to now reliably calculate EMA-solvent cloud-point curves, it is important to note that PMA densities calculated with these new pure component param-

eters are approximately 30% higher than experimental values.

The EMA₃₁-butane cloud-point curve is chosen for fitting $(u^\circ/k)_{\text{EMA}_{31}}$ because butane is a nonpolar solvent that is expected to interact mainly through dispersion and induction forces. The EMA₃₁-butane cloud-point curve, shown in Figure 1, increases in pressure as the temperature is decreased, a characteristic that must be captured for the modeling to be even qualitatively correct. Both $(u^\circ/k)_{\text{EMA}_{31}}$ and $k_{\text{butane-EMA}_{31}}$, the mixture parameter, are needed to obtain a good fit of the cloud-point curve. A low value of $(u^\circ/k)_{\text{EMA}_{31}}$ is required to keep the cloud-point curves at relatively low pressures at high temperatures, while a small positive value of $k_{\text{butane-EMA}_{31}}$ is required to impart significant curvature to the cloud-point curve. Without a positive value of $k_{\text{butane-EMA}_{31}}$ it is not possible to obtain a cloud-point curve with any significant curvature. Using these criteria, the best fit of the EMA₃₁-butane curve is obtained with $(u^\circ/k)_{\text{EMA}_{31}}$ equal to 220.0 K and k_{ij} equal to a constant value of 0.026. Using eqs. (4) and (9), the value of u°/k for PMA is 228.68 K, a much smaller value than that found by fitting density data for PMA. Now that the homopolymer values of u°/k for PE and PMA are known, eqs. (4) and (9) can be used to obtain the pure-component parameters for all of the EMA copolymers, as shown in Table IV.

COPOLYMER-ALKANE CALCULATIONS

Figure 2 shows the predicted cloud-point curves for PE, EMA₁₀, and EMA₃₁ in ethane. Hasch et al.²⁶ report that EMA₄₁ does not dissolve in ethane at 185°C and 2,800 bar probably due to the strong polar interactions between the 41 mol % methyl acrylate repeat units in the backbone of the copolymer. Calculations performed on the EMA₄₁-ethane system are in agreement with this observation, as they predict that a single phase will not occur at a constant

Table IV Parameters Calculated from Mixing Rules

Component	v^{oo} (cm ³ /mol)	m	u°/k (K)	ϵ/k (K)	v (cm ³ /mol)
PE	12.00	1,024.3	216.15	0	0
EMA ₁₀	12.00	866.3	217.39	0	0
EMA ₃₁	12.00	1,681.7	220.00	0	0
EMA ₄₁	12.00	1,523.7	221.24	0	0
PMA	12.00	1,019.2	228.68	0	0

Pure component parameters for PMA obtained from a fit of the EMA₃₁-butane cloud-point curve.

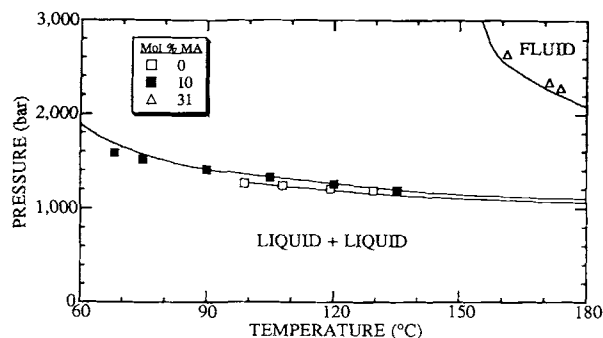


Figure 2 Calculated and experimental²⁶ cloud-point curves for PE, EMA₁₀, and EMA₃₁ in ethane. The symbols represent experimental data; the lines represent calculations obtained using SAFT. The calculations were performed with $k_{ij} = 0.025$ for the PE-ethane system, $k_{ij} = 0.026$ for the EMA₁₀-ethane system, and $k_{ij} = 0.038$ for the EMA₃₁-ethane system.

pressure of 2,500 bar until the temperature is above 210°C. The cloud-point pressures are predicted quantitatively over the entire temperature range with only one, temperature-independent k_{ij} equal to 0.025 for the PE-ethane system, 0.026 for the EMA₁₀-ethane system, and 0.038 for the EMA₃₁-ethane system. The mixture parameter is a small positive number for each of the EMA copolymers that increases in absolute value as the methyl acrylate content in the copolymer increases. The shape and locations of the calculated cloud-point curves are sensitive to small changes in the value of k_{ij} , particularly for the copolymers with high acrylate content. If k_{ij} is set equal to zero, the calculated cloud-point curves do not exhibit the correct qualitative behavior as the calculated curves do not exhibit any curvature. This result is unlike previously reported calculations¹³ for poly(ethylene-co-acrylic acid)-hydrocarbon systems, in which the correct shapes of the curves were predicted even when the mixture parameter is set equal to zero. For the acid copolymer-solvent mixtures, the calculations are dominated by the association term in SAFT that explicitly accounts for acid dimerization so that any corrections to the mean-field term only have a minor effect on the location of the cloud-point curve. However, SAFT does not specifically account for polar interactions present in EMA copolymers-solvent mixtures so that even small corrections to the mean-field term produce noticeable changes in the location of the cloud-point curves.

Figure 3 presents SAFT calculations for PE, EMA₁₀, and EMA₃₁ in propane. As with the EMA₄₁-ethane system, Hasch et al.²⁶ report that EMA₄₁ does not dissolve in propane at 185°C and 2,800 bar. Cal-

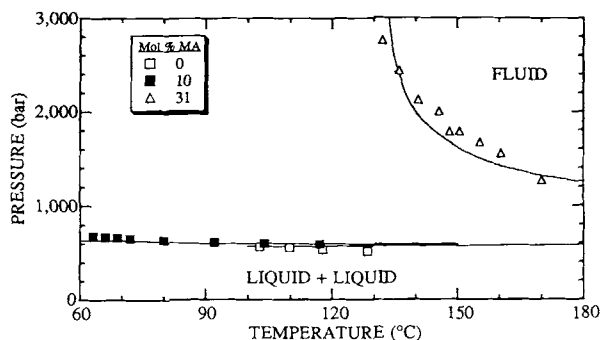


Figure 3 Calculated and experimental²⁶ cloud-point curves for PE, EMA₁₀, and EMA₃₁ in propane. The symbols represent experimental data; the lines represent calculations obtained using SAFT with $k_{ij} = 0.015$ for the PE-propane system, 0.015 for the EMA₁₀-propane system, and 0.029 for the EMA₃₁-propane system.

culations on the EMA₄₁-propane system corroborate this finding, because they predict that a single phase exists at 2,500 bar only at temperatures greater than 195°C. Figure 3 shows that the predicted cloud-point curves are in very good agreement with the experimental data at all temperatures with k_{ij} equal to 0.015 for the PE-propane system, 0.015 for the EMA₁₀-propane system, and 0.029 for the EMA₃₁-propane system. The trends observed in the mixture parameter and its effect on the shape and location of the cloud-point curves are similar to those observed in the EMA-ethane systems.

Figure 4 shows SAFT calculations for PE, EMA₃₁, and EMA₄₁ in butane. While all four EMA polymers are soluble in butane, the calculated and experimental data for the EMA₁₀-butane mixture are not

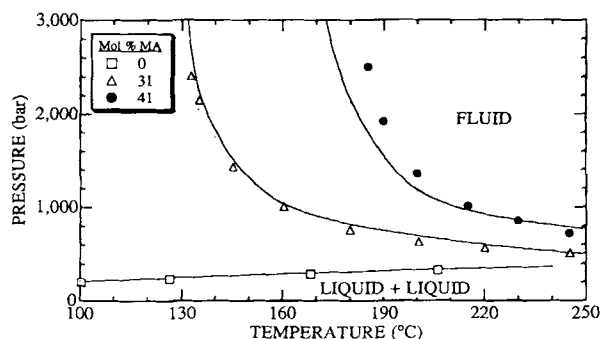


Figure 4 Calculated and experimental^{24,28} cloud-point curves for PE, EMA₃₁, and EMA₄₁ in butane. The symbols represent experimental data; the lines represent calculations obtained using SAFT with $k_{ij} = 0.008$ for the PE-butane system, 0.026 for the EMA₃₁-butane system, and 0.030 for the EMA₄₁-butane system.

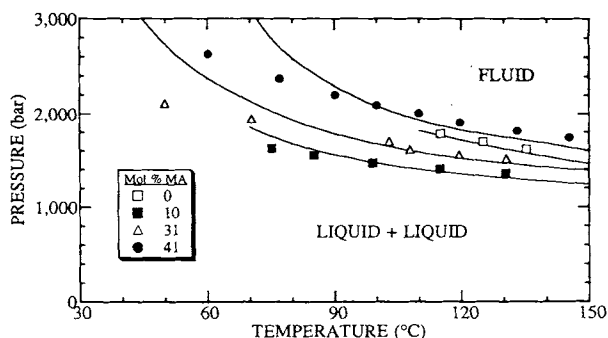


Figure 5 Calculated and experimental²⁶ cloud-point curves for PE, EMA₁₀, EMA₃₁, and EMA₄₁ in ethylene. The symbols represent experimental data; the lines represent calculations obtained using SAFT with $k_{ij} = 0.055$ for the PE-ethylene system, 0.048 for the EMA₁₀-ethylene system, 0.045 for the EMA₃₁-ethylene system, and 0.048 for the EMA₄₁-ethylene system.

shown to minimize clutter in the graph. The predicted cloud-point curves are in good quantitative agreement with the experimental results using k_{ij} values of 0.008 for the PE-butane and the EMA₁₀-butane systems, 0.026 for the EMA₃₁-butane system, and 0.030 for the EMA₄₁-butane. The trends seen in the value of the mixture parameter for EMA-butane systems also are observed for the EMA-ethane and EMA-propane systems.

COPOLYMER-ALKENE CALCULATIONS

As shown in the previous section, SAFT is able to reliably and quantitatively calculate the cloud-point pressures of EMA-alkane mixtures. In this section calculated cloud-point curves are compared to experimental data for EMA-alkene mixtures. As in the previous section, each copolymer-solvent cloud-point curve is fit with a single, temperature-independent mixture parameter.

Figure 5 shows predicted and experimental cloud-point curves for the EMA-ethylene system. The predicted cloud-point curves are in good agreement with the experimental data at high temperatures with k_{ij} values in the range of 0.050 ± 0.005 regardless of the acrylate content of the copolymer. It should be noted that ethylene dissolves EMA₄₁, but this copolymer is insoluble in nonpolar ethane at similar conditions.²⁶ At temperatures below $\sim 70^\circ\text{C}$, the predicted cloud-point pressures are greater than those observed for the high acrylate content copolymers. Because the mixture parameter does not change substantially with acrylate content, this suggests that a single averaged-value k_{ij} of 0.048

could be used to model all four EMA-ethylene mixtures. If this value of k_{ij} is used, the predicted EMA₃₁-ethylene cloud-point curve turns to higher pressures at $\sim 90^\circ\text{C}$ rather than at 70°C , and the predicted PE-ethylene cloud-point pressures are much too low. Apparently SAFT is not able to account for quadrupolar interactions between ethylene molecules and between ethylene and methyl acrylate repeat groups. The quadrupole of ethylene makes it a far better solvent for the polar, high-acrylate copolymers than the model predicts. However, this result is not particularly surprising given the lack of polarity-based terms in the SAFT theory.

Figure 6 presents predicted and experimental cloud-point data for the EMA-propylene system with k_{ij} equal to 0.030 for the PE-propylene system, 0.026 for the EMA₁₀-propylene system, 0.030 for the EMA₃₁-propylene system, and 0.033 for the EMA₄₁-propylene system. The trends observed in the calculated cloud-point curves are similar to those seen for EMA-ethylene mixtures. SAFT overpredicts the cloud-point pressures of EMA₃₁ and EMA₄₁-propylene mixtures at low temperatures. Once again, this result is likely due to SAFT's inability to account for the polar nature of propylene. Another similarity between the EMA-ethylene and EMA-propylene modeling is the behavior of the mixture parameter. The value of k_{ij} is almost constant over the entire range of copolymer compositions. If a constant value of k_{ij} is used to fit all four copolymer-propylene mixtures, the EMA₁₀-propylene cloud-point curve is located at pressures above the PE-propylene cloud-point curve. This is in direct contradiction to the experimental data, again emphasizing the argument that SAFT is unable to effec-

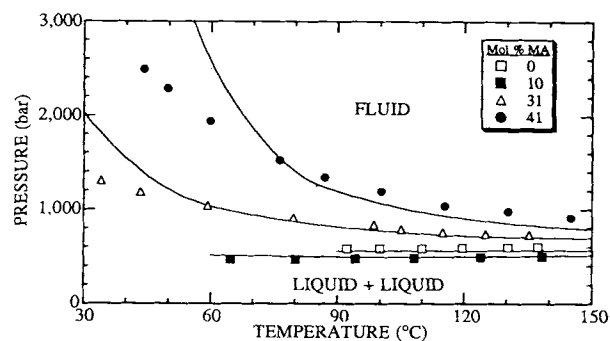


Figure 6 Calculated and experimental²⁶ cloud-point curves for PE, EMA₁₀, EMA₃₁, and EMA₄₁ in propylene. The symbols represent experimental data; the lines represent calculations obtained using SAFT with $k_{ij} = 0.030$ for the PE-propylene system, 0.026 for the EMA₁₀-propylene system, 0.030 for the EMA₃₁-propylene system, and 0.033 for the EMA₄₁-propylene system.

tively account for the impact of polar copolymer-polar solvent interactions on the phase behavior.

The final EMA-alkene system modeled is the EMA-butene system. Figure 7 shows calculated curves obtained using SAFT for PE, EMA₃₁, and EMA₄₁ in 1-butene. Calculations and data for the EMA₁₀-butene systems are omitted from the graph to avoid excessive clutter. The behavior of EMA-butene mixtures is somewhat similar to that seen with the other alkenes. The cloud-point pressures of high acrylate copolymer-alkene mixtures are overpredicted at low temperatures, although the extent of the overprediction is less in butene than in the other alkenes. The value of the mixture parameter becomes more positive as the acrylate content in the copolymer increases, which is unlike the behavior seen in the other EMA-alkene systems where the change in k_{ij} with acrylate content is very modest. This trend in k_{ij} is a bit misleading, however, as the PE-butene and EMA₁₀-butene cloud-point calculations are far less sensitive to changes in k_{ij} than the high acrylate-butene cloud-point calculations.

COPOLYMER-DME AND -CDFM CALCULATIONS

The previous two sections show that SAFT is able to effectively correlate the phase behavior of EMA-alkane and EMA-alkene mixtures. In this set of calculations, the phase behavior of EMA₃₁-DME and EMA₃₁-CDFM mixtures is calculated with SAFT. Figure 8 shows the calculated and experimental cloud-point curves for EMA₃₁-DME and EMA₃₁-CDFM mixtures with $k_{ij} = 0.010$ for EMA₃₁-DME

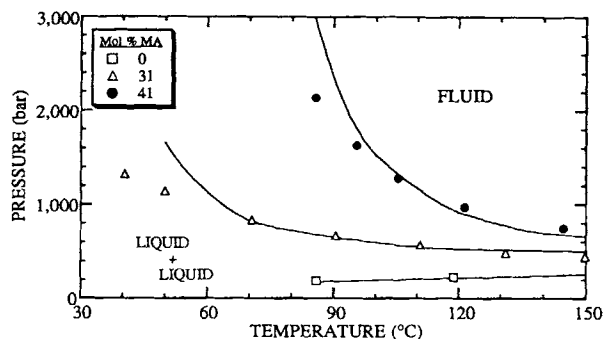


Figure 7 Calculated and experimental^{24,28} cloud-point curves for PE, EMA₁₀, EMA₃₁, and EMA₄₁ in 1-butene. The symbols represent experimental data; the lines represent calculations obtained using SAFT with $k_{ij} = 0.010$ for the PE-butene system, 0.021 for the EMA₃₁-butene system, and 0.025 for the EMA₄₁-butene system.

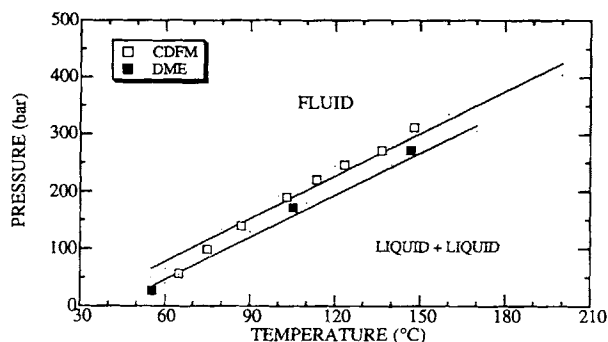


Figure 8 Calculated and experimental cloud-point curves for EMA₃₁ in dimethyl ether (DME) (original data) and chlorodifluoromethane (CDFM).²³ The symbols represent experimental data; the lines represent calculations obtained using SAFT with $k_{ij} = 0.010$ for the EMA₃₁-DME system and $k_{ij} = -0.020$ for the EMA₃₁-CDFM system.

and $k_{ij} = -0.020$ for EMA₃₁-CDFM. The cloud-point curves of these mixtures exhibit the characteristics of a lower critical solution temperature curve where the slope of the curves are positive in P-T space and they are located at pressures nearly an order of magnitude lower than those of the EMA₃₁-hydrocarbon mixtures. The predicted cloud-point curves are in good agreement with experimental data. From these calculations, it is apparent that SAFT is able to correlate phase behavior data of copolymer-solvent systems over a wide range of copolymer compositions and solvent types.

CONCLUSIONS

A method was presented for calculating the cloud-point behavior of nonpolar/polar copolymer-solvent mixtures using the SAFT equation of state. Unfortunately it is not possible to predict the cloud-point behavior for these polar mixtures with the SAFT equation. At present, it is only possible to correlate cloud-point data using this equation of state. Based on the calculations presented here, a very large value for the nonspecific, segment-segment interaction energy, u^0/k , in the mean-field dispersion term is obtained when homopolymer density data are fit to the equation of state. As a consequence of these excessively large values of u^0/k , the calculated cloud-point curves are not even in qualitative agreement with experimental data, despite the agreement of the calculated pure component densities with the experimental values. This limitation of SAFT was foreshadowed in the work of Huang and Radosz²⁰ who correlated the pure component values

Table V SAFT Mixture Parameters, k_{ij} , Determined for Systems in Study

	PE	EMA ₁₀	EMA ₃₁	EMA ₄₁
Ethane	0.025	0.026	0.038	—
Propane	0.015	0.015	0.029	—
Butane	0.008	0.008	0.026	0.030
Ethylene	0.055	0.048	0.045	0.048
Propylene	0.030	0.026	0.030	0.033
1-Butene	0.010	0.010	0.021	0.025
CDFM	—	—	-0.020	—
DME	—	—	0.010	—

for PE rather than using values fit to density data, because phase behavior calculations with these fitted parameters proved unsatisfactory.

In a study that used simulation data, Bokis et al.²⁷ show that the attractive term in SAFT does not scale with a constant value of the number of segments, m , particularly at low densities. Rather, they suggest that the attractive term should scale with a density-dependent scaling factor capable of accurately modeling the low-density region. Work is in progress to incorporate the findings of Bokis et al. into SAFT.

Of course, the other major limitation of the SAFT equation is that there is no explicit accounting for the effect of polar interactions. This is a major deficiency when working with the acrylate-rich copolymers addressed in this study, which is overcome only with the use of a k_{ij} value that varies with the acrylate content of the copolymer. Table V lists the values needed to obtain quantitative agreement between calculated and experimental results for the systems investigated in this study. Several trends are observed in these values. The value of k_{ij} for the PE-solvent system provides a fairly reasonable first estimate for the value needed for the other EMA-hydrocarbon solvent mixtures, except for butane. For the alkane systems investigated, the value of k_{ij} increases as the acrylate content increases from 0 to 41 mol %. However, for the alkene systems, the value of k_{ij} exhibits a minimum with methyl acrylate content. The high value of k_{ij} for the PE-alkene systems is not unexpected, because the solution contains a nonpolar polymer with a polar solvent. Likewise, the large values of k_{ij} needed with the EMA-alkane systems are also not unexpected, because the solution contains a polar copolymer with a nonpolar solvent. As methyl acrylate is added to the backbone of PE, the polarity increases and the alkene solvent and EMA copolymers with small amounts of methyl acrylate initially become more compatible; thus the value of k_{ij} decreases. However, as the acrylate con-

tent in the copolymer is further increased, the value of k_{ij} needed to obtain a good fit of the data also increases. Notice that the value of k_{ij} decreases for PE and for the EMA copolymers as the molecular weight of the solvent increases. As noted earlier, the primary role of k_{ij} apparently is to impart curvature to the cloud-point curve. At this point in time, more calculational studies are needed to develop a correlation for k_{ij} as a function of copolymer composition.

Regardless of its deficiencies, the SAFT equation of state provides results that are in marked improvement when compared to, for example, the Sanchez-Lacombe equation of state. Earlier attempts to model the simple PE-solvent systems using the Sanchez-Lacombe equation of state²⁶ required a minimum of three adjustable parameters for each curve to obtain quantitative agreement with the data. Further work is warranted to use SAFT in a correlative manner to calculate cloud-point behavior of copolymer-solvent mixtures. There is no question that, at present, some binary copolymer-solvent data are needed to apply the SAFT equation. In addition, the pure component polymer densities predicted by SAFT using parameters fitted to cloud-point data are 30% too high. While this approach is not predictive, it does provide a valuable correlating tool for calculating the phase behavior of systems based on a limited amount of experimental data.

The authors acknowledge the National Science Foundation for support of this project under Grant CTS-9122003. They also acknowledge the technical help of Dr. Markus Busch of the Institut für Physikalische Chemie, Universität Göttingen, who assisted in some of the programming.

REFERENCES

1. R. L. Boysen, in *Kirk-Othmer Encyclopedia of Chemical Technology*, M. Grayson, Ed., Wiley, New York, 1981.

2. W. G. Chapman, K. E. Gubbins, G. Jackson, and M. Radosz, *Fluid Phase Equilibrium*, **52**, 31 (1989).
3. M. S. Wertheim, *J. Stat. Phys.*, **35**, 19 (1984).
4. M. S. Wertheim, *J. Stat. Phys.*, **35**, 35 (1984).
5. M. S. Wertheim, *J. Stat. Phys.*, **42**, 459 (1986).
6. M. S. Wertheim, *J. Stat. Phys.*, **42**, 477 (1986).
7. S.-J. Chen, I. G. Economou, and M. Radosz, *Macromolecules*, **25**, 4987 (1992).
8. S.-J. Chen, I. G. Economou, and M. Radosz, *Fluid Phase Equilibrium*, **83**, 391 (1993).
9. C. J. Gregg, S.-J. Chen, F. P. Stein, and M. Radosz, *Fluid Phase Equilibrium*, **83**, 375 (1993).
10. C. J. Gregg, S.-J. Chen, F. P. Stein, and M. Radosz, *Macromolecules*, **27**, 4972 (1994).
11. C. J. Gregg, S.-J. Chen, F. P. Stein, and M. Radosz, *Macromolecules*, **27**, 4980 (1994).
12. J. Suresh, R. Enick, and E. Beckman, *Macromolecules*, **27**, 348 (1994).
13. B. M. Hasch and M. A. McHugh, *J. Polym. Sci. Part B: Polym. Phys.*, **33**, 715 (1995).
14. D. Pradhan, C. Chen, and M. Radosz, *I & E.C. Research*, **33**, 1984 (1994).
15. M. A. LoStracco, S.-H. Lee, and M. A. McHugh, *Polymer*, **35**, 3272 (1994).
16. N. F. Carnahan and K. E. Starling, *J. Chem. Phys.*, **51**, 635 (1969).
17. W. G. Chapman, K. E. Gubbins, G. Jackson, and M. Radosz, *Ind. Eng. Chem. Res.*, **29**, 1709 (1990).
18. B. J. Alder, D. A. Young, and M. A. Mark, *J. Chem. Phys.*, **56**, 3013 (1972).
19. S. Beret and J. M. Prausnitz, *AIChE J.*, **21**, 1123 (1975).
20. S. H. Huang and M. Radosz, *Ind. Eng. Chem. Res.*, **29**, 2284 (1990).
21. S. H. Huang and M. Radosz, *Ind. Eng. Chem. Res.*, **30**, 1994 (1991).
22. C. G. Panayiotou, *Makromol. Chem.*, **188**, 2733 (1987).
23. M. A. Meilchen, B. M. Hasch, and M. A. McHugh, *Macromolecules*, **24**, 4874 (1991).
24. S.-H. Lee, M. A. LoStracco, B. M. Hasch, and M. A. McHugh, *J. Phys. Chem.*, **98**, 4055 (1994).
25. P. A. Rodgers, *J. Appl. Poly. Sci.*, **48**, 1061 (1993).
26. B. M. Hasch, M. A. Meilchen, S.-H. Lee, and M. A. McHugh, *J. Polym. Sci. Part B: Polym. Phys.*, **30**, 1365 (1992).
27. C. P. Bokis, M. D. Donohue, and C. K. Hall, *Ind. Eng. Chem. Res.*, **33**, 1290 (1994).
28. J. A. Pratt, S.-H. Lee, and M. A. McHugh, *J. Appl. Polym. Sci.*, **49**, 953 (1993).

Received May 1, 1995

Accepted July 13, 1995